Journal of Neuroscience Methods 185 (2009) 125–132

Contents lists available at ScienceDirect

Journal of Neuroscience Methods

journal homepage: www.elsevier.com/locate/jneumeth

Approximate average head models for EEG source imaging

Pedro A. Valdés-Hernández[a,*,1], Nicolás von Ellenrieder[b,1], Alejandro Ojeda-Gonzalez[a], Silvia Kochen[c], Yasser Alemán-Gómez[a], Carlos Muravchik[b], Pedro A. Valdés-Sosa[a]

[a] Neuroimaging Department, Cuban Neuroscience Center, Havana, Cuba
[b] Laboratory of Industrial Electronics, Control and Instrumentation, National University of La Plata, La Plata, Argentina
[c] Epilepsy Center, IBCN - CONICET - University of Buenos Aires, Buenos Aires, Argentina

ARTICLE INFO

Article history:
Received 28 July 2009
Received in revised form 1 September 2009
Accepted 1 September 2009

Keywords:
Approximate head model
Average
Electrode measurement
Thin Plate Spline
BEM
Lead field
sLORETA
MNI
EEG Cuban Brain Mapping Project

ABSTRACT

We examine the performance of approximate models (AM) of the head in solving the EEG inverse problem. The AM are needed when the individual's MRI is not available. We simulate the electric potential distribution generated by cortical sources for a large sample of 305 subjects, and solve the inverse problem with AM. Statistical comparisons are carried out with the distribution of the localization errors. We propose several new AM. These are the average of many individual realistic MRI-based models, such as surface-based models or lead fields. We demonstrate that the lead fields of the AM should be calculated considering source moments not constrained to be normal to the cortex. We also show that the imperfect anatomical correspondence between all cortices is the most important cause of localization errors. Our average models perform better than a random individual model or the usual average model in the MNI space. We also show that a classification based on race and gender or head size before averaging does not significantly improve the results. Our average models are slightly better than an existing AM with shape guided by measured individual electrode positions, and have the advantage of not requiring such measurements. Among the studied models, the Average Lead Field seems the most convenient tool in large and systematical clinical and research studies demanding EEG source localization, when MRI are unavailable. This AM does not need a strict alignment between head models, and can therefore be easily achieved for any type of head modeling approach.

1. Introduction

In Electromagnetic Source Imaging (ESI), the smallest source localization error is achieved when the physical properties of the head are modeled with the information provided by the individual's Magnetic Resonance Image (MRI) (Huiskamp et al., 1999; Henson et al., 2009). However in some cases an MRI system is not available or EEG related studies with a large number of individuals make MR acquisition unpractical. In this work we are interested in finding the best possible approximation of the individual head model when the MRI-based head model is unknown. We quantify the performance of a head model by the error in the estimation of the source position. The value of this error would be helpful to decide in which situations an approximate model is acceptable.

The simplest and worst approximate head model is a set of spheres representing the boundaries of different tissue domains of the head with homogeneous physical conductivities (de Munck and Peters, 1993; Ermer et al., 2001). A further improvement is achieved by using realistically shaped head models based on standard MRIs, such as the average image provided by the Montreal Neurological Institute (ICBM-152), as proposed in (Fuchs et al., 2002). However the ICBM-152, as being an average of 9 parameter-based affine coregistered individual MRIs, presents a coarse level of anatomical detail. This compromises the accuracy of some volumetric piecewise head modeling methods such as the Finite Element Method (FEM) (Wolters et al., 2006) and the Finite Difference Method (FDM) (Neilson, 2003). Alternatively finer detailed standard MRIs could be used, e.g. the average of 27 MRIs from a single individual in MNI space (MNI-27) (Collins et al., 1998), or the average of different individual MRIs that have been nonlinearly coregistered to a common stereotaxic space (ICBM-452) (Mazziotta et al., 2001). However, these standard MRIs are far from being representative of a target population in the sense of shape since they are registered to the MNI space. No matter the level of anatomical detail achieved, a wrong shaped approximation is a major cause of localization errors in ESI, as shown in (von Ellenrieder et al., 2009). Therefore, reducing the shape differences between the approximate and individual head models is a prime goal in improving the performance of the approximate head models in ESI.

* Corresponding author at: Neuroimaging Department, Cuban Neuroscience Center, Ave 25, Esq. 158, #15202, PO Box 6412/6414, Cubanacán, Playa, Havana, Cuba. Tel.: +53 7 208 4460; fax: +53 7 208 6707.
E-mail address: multivac@cneuro.edu.cu (P.A. Valdés-Hernández).
[1] Both authors contributed equally.

0165-0270/$ – see front matter © 2009 Elsevier B.V. All rights reserved.
doi:10.1016/j.jneumeth.2009.09.005

The MNI-shape drawback has only been dealt with in (Darvas et al., 2006), where the ICBM-152 was warped to the individual space through a nonlinear Thin Plate Spline (TPS) transformation. This TPS was estimated by matching the predefined electrode positions in the scalp of the ICBM-152 (the template) to those measured in the individual. The TPS head model has two problems: (1) the shape improvement is, by definition, more effective toward the scalp, inheriting the defects of the chosen template model; (2) the individual electrode positions have to be measured manually (de Munck et al., 1991), or with a Polhemus device (Lamm et al., 2001) or by other methods (Le et al., 1998).

In this paper, we propose new approximate head models that do not require the measurement of the electrode positions. These methods are also designed to be, from a statistical point of view, closer in shape to the individual unknown head model than the MNI-shaped and TPS head models. We are interested in reducing the localization error by modifying only the shape. Therefore, we work with head models consisting of a set of surfaces defining the boundary of nested homogeneous and isotropic compartments, as proposed elsewhere (Hämäläinen and Sarvas, 1989; de Munck, 1992; Ermer et al., 2001; Fuchs et al., 1998, 2001, 2002; von Ellenrieder et al., 2009), thus adopting the Boundary Element Method (BEM) to solve the Forward Problem of the EEG (de Munck, 1992), i.e. the calculation of the lead field matrix. The first of our proposed approximate head model is an estimate of the shape centroid of the target population built with the head models defined from 305 MRIs drawn from the Cuban Human Brain Mapping Project. This head model is the closest in shape to all the individual head models. In Appendix A, we demonstrate that the simple surface element wise average can readily substitute for this head model.

Therefore an estimate of the centroid head model is only easily achievable for surface-based head models. This simple average concept cannot be extended straightforwardly to more heterogeneous head models, such as FEM or FDT. The centroid estimate of these type of head models involves complicated inter-subject registration pipelines (see for example, Guimond, 2000; Christensen et al., 2006 and Appendix A), requiring high dimensional nonlinear registration methods to achieve detailed images. Additionally, they are not easy to update with newer models. Therefore, as a new alternative, we investigate the use of the direct average of the lead fields of the subjects of the sample. This model only requires very simple transformations to align head models before calculating the lead fields and its use is computationally inexpensive. The Average Lead Field has to be calculated for predetermined electrode montages. This is well suited for systematical studies involving a large sample of individuals.

Further approaches are considered in this work such as partial head model averages clustered according to race, sex or head size of the individuals. With this we investigate whether the knowledge of these individual externals characteristics, which are easy to determine, can be used to decrease the source localization error.

The first idea that would come into mind when the individual's MRI head model is not available is using any head model at hand, which is equivalent to taking that defined from a random disparate subject. In fact some works in the literature used this approach, e.g. the Collins head in (Trujillo-Barreto et al., 2008). We also evaluate in this work how prejudicial this can be for ESI.

We evaluate the improvement in the performance of all the proposed head models, and compare them with existing approaches in the literature, adapted to our dataset, i.e. the MNI-shaped model and its TPS version. Finally we also investigate a possible improvement by using a TPS transformation of the Average Surface model. We consider that this improvement should be considerable to make the measurement of electrode positions worthwhile.

Without loss of generality, the algorithms for the EEG Inverse Problem are chosen to yield a null expected localization error when the individual MRI head models are used. In this way the localization error obtained when using an approximate head model will be caused only by its difference from the individual head models.

2. Materials and methods

The head model we adopted has three parts: (1) the volume conductor model, representing the physical properties of the head, (2) the cortical surface, providing the possible location and orientation of the sources of the EEG and (3) the fiducials on the outer surface of the skin, which serve as guidelines to locate the positions of the electrodes (where the EEG is measured). The fiducials can include the electrode positions as is the case of the TPS-based head models.

In this work we deal with the following hypothetical experimental situation. Someone measures the scalp electrical potential in an individual without MRI. Since he/she wants to obtain the sources of the measured EEG he/she is forced to use an approximate head model for ESI. Using the fiducials as guidelines, an electrode set is placed on the approximate scalp in an attempt to reproduce the same anatomical locations where EEG was measured in the individual scalp. Then the forward problem and inverse problems of the EEG are solved. In this section we test the performance of several approximate head models in ESI.

The test is done as follows. We simulated the expected electric potential measurements generated by known sources. This is done with the individual's MRI head model. Then we solve the inverse problem, i.e. source localization, using the approximate head model, and compare the estimated sources with the simulated ones by means of the localization error. This is carried out for a subset of 305 individuals of the Cuban Human Brain Mapping Project (CHBMP) in a leave one out statistical procedure, i.e. each subject is taken to simulate sources and EEG whereas the remaining 304 head models are taken to achieve the approximate model. This procedure yields 305 localization errors for each approximate head model.

The CHBMP is composed by a large sample of subjects of the Cuban population, randomly selected from the Cuban National ID registry, who were submitted to neuropsychiatrical and neuropsychological tests. Those who were considered by experts as healthy subjects were included in the database, after informed consent.

2.1. MRI-based head models

We adopted a layered model for the head, with three nested compartments of constant isotropic conductivity representing the brain, skull, and skin tissues. The electrical conductivity values are 0.33 S/m for the brain and skin and 0.022 S/m for the skull. The 1/15 skull/skin conductivity ratio is supported by recent studies (Oostendorp et al., 2000; Wendel and Malmivuo, 2006; Zhang et al., 2006). The shape of these layers was obtained from magnetic resonance images (MRIs) of the subjects. These MRIs were obtained using a Siemens Symphony 1.5 T system, consisting in a set of 3D MPRAGE T1-weighted images of dimensions $160 \times 256 \times 256$, and $1\,\text{mm} \times 1\,\text{mm} \times 1\,\text{mm}$ voxel size, TR = 100 ms, TE = 3.3 ms, and TI = 1100 ms.

The images were segmented into brain, skull and skin using the best outcome, according to an expert's criterion, between betsurf, a tool of the FSL software package (Jenkinson et al., 2005), and BrainSuite2 (Shattuck and Leahy, 2002). They yielded three surfaces, characterized by tessellations (nodes and triangles), for each subject: *inskull* (brain/skull interface), *outskull* (skull/skin interface) and *scalp* (skin/air interface). However, we discarded the extracted inskulls for both softwares due to their very low quality, a conse-

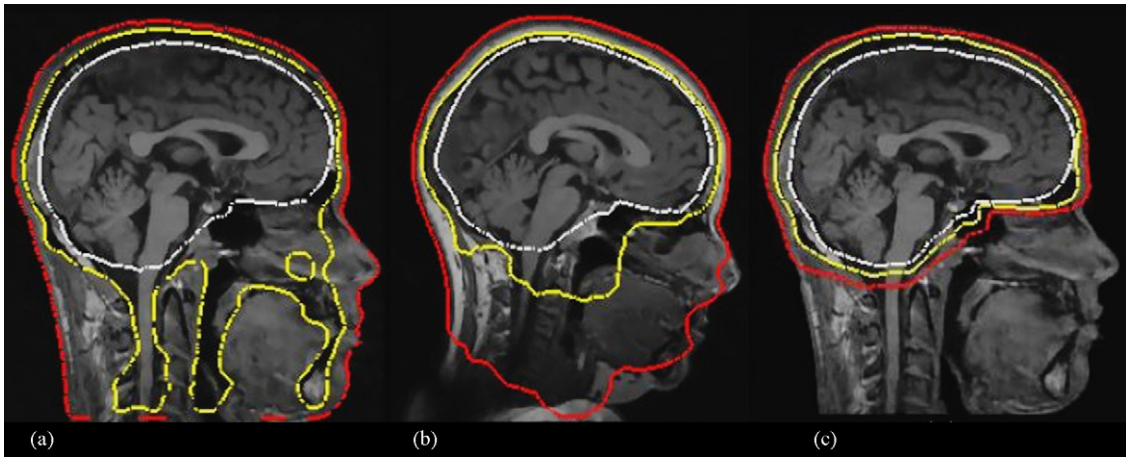

Fig. 1. Inskull (white), outskull (yellow) and scalp (red) extracted with (a) BrainSuite2 and (b) FSL BET2 (betsurf). The inferior part of corresponding outskulls and scalps is different for both softwares. (c) Outskull and scalp were modified to have uniform shape irrespective of the software used. We ensured this by replacing the parts of skull and skin layers below the plane defined by the fiducials by layers of 6 mm and 8 mm thicknesses respectively. The transition between the reconstructed and unchanged parts was linearly smoothed. (For interpretation of the references to color in this figure legend, the reader is referred to the web version of the article.)

quence of the low contrast between cerebrospinal fluid and skull in a T1-weighted image. Instead we took the inskull corresponding to the ICBM-152 template warped to individual space. This was done with the transformation obtained by registering the skull-stripped T1-weighted image to the skull-stripped ICBM-152 template with a nonlinear registration method (Thirion, 1998).

The head model surfaces were registered to a common coordinate system with the origin 50 mm above the intersection between the segment joining the left and right preauricular points and a line perpendicular to this segment passing through the nasion. This has two purposes. (1) Outskull and scalp provided by the software packages differ in the inferior part of the model, e.g. in the inclusion of the neck in the model, as shown in Fig. 1. We modified these surfaces in order to obtain a uniform shape for all the subjects. To accomplish this we replaced the parts of the skull and skin below the plane defined by the fiducials by layers of constant thickness of 6 mm and 8 mm respectively, which are the average thicknesses of these tissue domains in our sample. The transition from the reconstructed to the unchanged parts of the layers was linearly smoothed to avoid abrupt changes (see Fig. 1). (2) To allow a description of the surfaces as Spherical Harmonics decompositions, facilitating their tessellation (van't Ent et al., 2001) and establishing a correspondence between surfaces which is mandatory for inter-subject averaging and layer thickness calculations.

Each surface S was represented as the set of points:

$$S \equiv \left\{ (\varphi, \theta, r) : r = \sum_{l=0}^{N_A} \sum_{m=-l}^{l} a_{lm} Y_{lm}(\varphi, \theta) \right\} \quad (1)$$

where (φ,θ,r) are the azimuth, elevation and distance to the origin of the points. The functions Y_{lm} are the Spherical Harmonics (Abramovitz and Stegun, 2009) and $N_A = 30$ is the order of the decomposition which lead to $(N_A + 1)^2 = 961$ terms. The coefficients a_{lm} are obtained by minimizing the distance between S and the set of nodes describing the surface extracted by the software packages.

The individual positions of the preauricular points and the nasion, mentioned above, were achieved by nonlinearly transforming their positions in the ICBM-152 template to the individual space and projecting them onto the individual scalp. The transformation was obtained by nonlinearly normalizing the T1-weighted image to the ICBM-152 template using SPM5 with cutoff = 25 mm (Ashburner and Friston, 1999).

We assumed that the sources of electrical activity are restricted to the neocortical layer, specifically its middle surface, as being the most representative location of cortical activity. We extracted this surface with the CIVET software package (Robbins, 2003; Ad-Dab'bagh et al., 2006). The output surfaces had more than 80,000 nodes which were subsampled to 10,000. This software provides inter-subject anatomical correspondence between surfaces nodes, which is needed to average head models and to provide a meaningful anatomical localization error in our simulations.

2.2. Source simulation

Using the MRI-based volume conductor and cortex models, we simulated, for each subject, the "actual" electric potential generated by a known dipolar source in each of the 10,000 nodes of the cortical surface. The dipolar moment was oriented along the normal vector of the cortex, according to the behavior of the electrical activity in this surface (Dale and Sereno, 1993; Malmivuo and Plonsey, 1995). This simulation consists in solving the forward problem of the EEG, i.e. the quasistatic Maxwell equations in the head.

The electrical potentials are measured in a particular set of electrodes. We use the montage (120 electrodes) shown in Fig. 2. This montage was manually placed in the ICBM-152 template. We wanted to achieve the same situation across subjects, avoiding possible errors in electrode positioning; thus each individual montage was obtained by transforming the ICBM-152 montage to each individual space and projecting onto the individual scalp. We used the same SPM transformations previously used to obtain nasion and preauriculars.

We solved the Forward Problem of the EEG with the BEM (de Munck, 1992). A linear variation of the electric potential was assumed through the triangular elements of the interlayer surfaces (de Munck, 1992). To avoid numerical problems due to the low electric conductivity of the skull we adopted the Isolated Problem Approach (Meijs et al., 1989). Scalp and outskull were tessellated into 5120 triangular elements, and the inskull tessellated in at least 10,240 triangular elements. The procedure to tessellate inskull included a local refinement where this surface is too close to the cortical surface, in order to have triangle sides shorter than 1.5 times the local distance between both surfaces. This is done to keep valid the linear approximation of the electric potential (Haueisen et al., 1997).

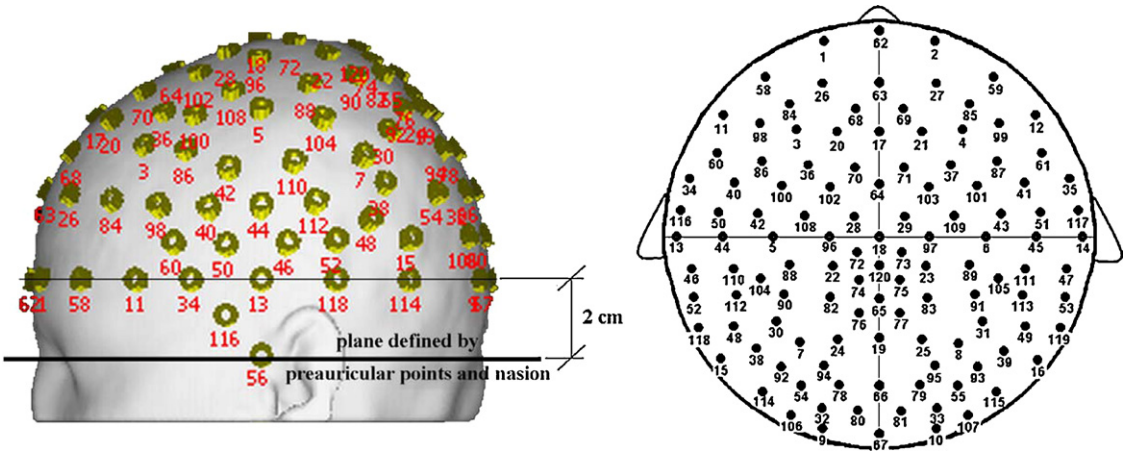

Fig. 2. Electrode montage used in this paper (120 electrodes). This montage was manually placed on the ICBM-152 template scalp.

2.3. Source estimation

We use the approximate head models for the source estimation. These are described in the next subsection.

In ESI methods, the source estimation from the measurements, i.e. the inverse problem of the EEG, requires as an intermediate step the solution of the EEG forward problem, i.e. the calculation of the lead field matrix. We did this for the approximate head models with BEM, with a tessellation coarser than the one used to simulate scalp electrical potentials, i.e. with both scalp and outskull tessellated into 2560 triangular elements, and inskull into at least 5120 triangular elements. The local refinement yielded triangle sides shorter than two times the local distance between inskull and cortex. These coarser tessellations are adopted to reduce the computational load associated with the construction of the approximate models, as well as to determine if such tessellations are fine enough for good quality ESI results.

In the actual experimental situation, the electrodes (shown in Fig. 2 for our case) should be placed in the approximate scalp according to the fiducials of the approximate head model in a manner decided by the experimentalist, attempting to achieve the same individual's measurement positions. There might be several sets of fiducials and strategies to place electrodes. For example, the fiducials can be the nasion, inion, vertex and preauricular points, or measured electrode positions itself; while electrode positions can be achieved by transforming those defined in the standard space (ICBM-152 for our case) to the approximate space using a fiducials-based affine transformation, a TPS transformation or a manual procedure. Apart from the expected errors due to shape approximation, all of these approaches are affected by additional errors associated with the nature of the electrode positioning procedure itself. In this work, we are not interested in evaluating these effects on source reconstruction errors since fortunately the former is not much sensible to changes of the latter (Wang and Gotman, 2001). Therefore, in the simulations of this paper, we deliberately take advantage of the known anatomical correspondence existing between the subjects' electrode sets of the database (achieved by nonlinear registration above) to guarantee the best anatomical correspondence between the approximate and individual electrode sets. The exact way this is achieved for each approximate head model is described in the next subsection.

Although a dipole was simulated with its moment constrained to the normal of the true cortex, the lead field for the estimation can be calculated with and without constraining the moment to the normals of the approximate cortex. We test both approaches since we believe the constraint might cause larger localization errors. We explain this as follows. Although the true and the approximate cortices are anatomically registered each other, their normals do not necessarily point in the same direction with respect to the electrode montage. Thus a dipole in the same node of both surfaces, with its moment constrained to the normal direction, might yield very different electrical potential topographies. With the moment unconstrained, the estimated dipole can simultaneously be located at the simulation node and have a direction that generates a scalp electrical potential topography much more similar to the simulated one.

In this work we use sLORETA (Pascual-Marqui, 2002) to estimate the sources. The useful information of sLORETA is the estimated position. Although the estimation of dipolar moment orientation and intensity is also part of the inverse problem, we believe that the most important quality of models and algorithms is to correctly localize the source of brain activity. Therefore we shall only consider the localization error as the measure of source reconstruction error. We define the localization error as the Euclidean distance between the positions of the nodes, measured in the true cortex, of both the simulated and maximum of the estimated sources. Note that we are measuring distances between anatomically equivalent sources, i.e. zero localization error means that both sources have the same anatomical "location", even though the true source is located in the individual cortex, and the estimated one in the approximate cortex. We note that we could use geodesic distance between points as a measure of localization error, which for simplicity sake was not done in this paper.

When no noise is present in the measurements, sLORETA yields zero localization error when using the actual head model. This situation is therefore beneficial to evaluate the performance of the approximate head models since the only cause of localization errors are differences between approximate and actual head models.

For a tested model we have 305 subjects and 10,000 different source locations, yielding a total of more than three million inverse problem results. We report in this work the mean localization error (MLE) pooled over subjects and source positions, and the 95% quantile (q95) of these errors.

Additionally, we compare the performance of two head models in source reconstruction by statistically comparing the distributions of 305 average localization errors (ALE) for both models. This is a partial average through all source positions. We use the Kolmogorov–Smirnov (KS) test at 5% significance level. The null hypothesis is that the average error distributions are the same for both head models. The KS is a nonparametric test which makes no assumptions about the distributions.

2.4. Approximate head models

2.4.1. Existing approaches

- *Random*: In this paper we choose this model randomly from the CHBM database. Consequently with the desired "electrode anatomical correspondence" condition described above, we use the electrode positions previously calculated for this randomly chosen subject.
- *CHBM-305*: Since we want to compare our proposed approximate head models to those based on MNI-shaped standard MRIs, we define the equivalent MNI-shaped head model (Fuchs et al., 2002) for our database. This is an average of the 305 MRI-based models following the same procedures followed to construct the ICBM-152 standard MRI. The electrode montage is shown in Fig. 2.
- *CHBM-305 TPS*: This is the Thin Plate Spline transformation of the CHBM-305, as defined by (Darvas et al., 2006).
- *Random TPS*: This is the Thin Plate Spline transformation of the Random model.

2.4.2. New approaches

- *Average surface*: We provide an estimate of the centroid head model, in the sense of shape, of the target population. It is obtained by averaging, through subjects, the coefficients, a_{lm}, in Eq. (1) of the Spherical Harmonics decompositions. The average cortical surface is obtained by averaging the corresponding cortical node positions. This can be done since they are in anatomical correspondence and all the head models were previously oriented to a fiducials-based coordinate system. As demonstrated in Appendix A, the Average Surface model is an estimate of the centroid shape of a population. The electrode positions for this approximate head model are simply the average of all corresponding electrode positions across subjects projected to the Average Scalp. This provides an "average electrode anatomical correspondence" between head models, as desired.
- *Average Lead Field*: Since all the parts of our head models are in anatomical correspondence we can average the lead fields. Although the relation between model shape and lead field is not linear, the head shape variations through individuals are small enough to consider their effect on the lead field as approximately linear. Therefore the Average Lead Field should produce similar results to the Average Surface model. For our analyses, we only need to define the Average Lead Field for the electrode montage considered in this work. For the lead fields with the source moments constrained to the normal direction of the cortical surface the Average Lead Field does not need a previous alignment between head models since the lead field is theoretically invariant under rigid body transformations. This is not the case of the unconstrained case. Notwithstanding, we shall consider as sufficient the landmark-based alignment previously performed to the individuals head models to make possible the construction of the Average Lead Field.

2.4.3. Classifications according to sex, race and head size

Additionally we tried averaging models of subjects after a classification. The Average Lead Field of the group where the individual under study classifies is used to solve the inverse problem. We tried two classifications, one according to the race and gender (RGC) of the subjects, and the other based on the "size" of the head (HSC). For RGC we clustered the subjects in four categories; 93 women, 89 white men, 71 black men, and 51 mulatto men. One subject from another race was excluded from this analysis. For HSC we used two features that are easy to measure: the nasion–inion distance and the distance between the preauricular points. We classified the subjects in six HSC groups, using the *K*-means algorithm, which minimizes the variance in the groups. The number of subjects in the resulting groups was 10, 45, 54, 60, 62, and 74. To determine whether the proposed classifications improve ESI results, we tested with control groups of the same number of subjects than in the RGC and HSC, but drawn randomly from the database.

2.4.4. Average surface TPS

This is the Thin Plate Spline transformation to the Average Surface model.

3. Results

In this section we first examine the validity of some of the assumptions we made in the definition and construction of the head models. Then we discuss and compare the performance of our proposed approximate models with existing approaches in the literature.

3.1. Validation of some of the assumptions made in this paper

3.1.1. The Spherical Harmonic approximation

To evaluate the accuracy of Spherical Harmonic (SH) approximations we first calculated the distance between the *i*th point of an SH surface $(\varphi^i, \theta^i, r^i_{\mathrm{SH}})$ and its corresponding point in the actual surface $(\varphi^i, \theta^i, r^i_{\mathrm{ACTUAL}})$, and then we averaged across all points:

$$\varepsilon = \sum_i \left| r^i_{\mathrm{ACTUAL}} - r^i_{\mathrm{SH}} \right|, \tag{2}$$

where $|a|$ is the absolute value of a.

The values of ε are 0.53 mm, 0.25 mm and 0.09 mm for inskull, outskull and scalp respectively. These are negligible compared to the average radius of these surfaces in the Surface Average model, which are 71.6 mm, 76.9 mm and 85.6 mm respectively. Also, as demonstrated in (von Ellenrieder et al., 2006), errors below 1 mm do not influence on the EEG Inverse Problem.

3.1.2. The coarse tessellation approximation

The lead fields for source estimation are based on a tessellation coarser than that used for source simulation. The effect of this on the localization error was achieved by solving the inverse problem with the actual MRI-based head model of the individual, but using the lead field computed with the coarser tessellation. The Mean Localization Error (MLE) across subjects and source positions, and the 95% quantile of the localization errors (q95) were 0.13 mm and 1.03 mm respectively. We consider these values as negligible compared to the localization errors when using approximate head models. This validates the use of the coarser tessellation for source estimation.

3.1.3. The averaging approximation

It should be noted that most of the tested methods involve averaging among all the individual models, i.e. including the individual under study, which is supposed to be left out according to the jack-knife procedure. This can be accepted if we assume that, for the large number of subjects considered, the 305 jack-knife averages of the 304 remaining head models are very similar to the average of the 305 head models. Indeed, Table 1 shows very similar results for the MLE and q95 of both approaches. Moreover the KS test shows that the null hypothesis, of identical distributions of Average Localization Errors (ALE) through source positions, cannot be discarded ($p = 0.999$). We make an exception however for the groups classified by gender, race or size, where the number of subjects is, in some cases, much lower.

Table 1
Mean Localization Error (MLE) and 95% quantile (q95) for the approximate head models. Except the shadowed approximate head models, the lead fields were calculated with the source moments not constrained to the normals of the cortex model.

Head model	Mean localization error—MLE [mm]	95% quantile e95 [mm]
Individual coarser tessellation	0.1	1.0
Average Lead Field (moments constrained to the cortex normals)	8.2	18.9
Average Lead Field (jack-knife 304 subjects)	5.9	13.0
Average Lead Field (305 subjects)	5.9	13.0
Average surface	5.9	13.0
Random	8.8	18.2
CHBM-305	6.4	13.5
Thin Plate Spline on random	8.3	17.5
Thin Plate Spline on CHBM-305	6.0	13.1
Thin Plate Spline on average surface	5.8	12.9
Race-gender group	5.9	13.0
Race-gender control group (the same size with randomly selected members)	6.0	13.1
Head size group	5.9	13.0
Head size control group (the same size with randomly selected members)	6.0	13.1

3.1.4. Dipole moment constraint

Table 1 shows that the Average Lead Field with the dipole moments *not* constrained to the normals of the approximate cortex outperforms the constrained case. The KS test confirmed this fact ($p \approx 0$). This is in agreement with the results found in (Henson et al., 2009) for individual head models in Magnetoencephalography (MEG). In that paper, the unrestricted case showed better results for L2-Minimum Norm inverse solutions. Note that the sLORETA solution is precisely constructed from this type of solution (Pascual-Marqui, 2002). Based on this result we test the performance of all the approximate head models with the unconstrained approach.

3.2. Comparison between the performance of approximate head models in ESI

Both the MLE and q95 are presented in Table 1 for all the new approximate head models, i.e. the Average Surface, the Average Lead Field, the TPS of the Average Surface and for those already reported, i.e. the CHBM-305, the Random and their corresponding TPS models. It can be seen that the performance of the Average models is better than that of the MNI-shaped model and the Random model, as expected due to their low representativeness, in the sense of shape, of the target population.

The KS test did not reject equal distributions of the ALE of the Average Surface and the Average Lead Field models ($p = 0.99992$). The MLE for both models is near 6 mm, and the q95 around 13 mm. Fig. 3 shows, for the Average Lead Field, the average localization error among the 305 subjects for each source location. It can be seen that this error is lower for deeper sources, and higher for sources near the inskull surface.

The classification of average models in RGC and HSC groups yields no improvement in source reconstruction, as can be seen in Table 1. The difference between these groups and their corresponding random control groups is not significant, according to the KS test ($p = 0.25$ and $p = 0.39$ for the RGC and HSC respectively).

The use of known measured electrode positions, via the TPS transformation, improves the MLE of the CHBM-305 model ($p = 1.5 \times 10^{-13}$), reproducing the results of (Darvas et al., 2006). An additional result is elucidated from the analysis of the improvements provided by the TPS transformed models with respect to their templates (Random, CHBM-305 and Average Surface): the better the template model, the lesser the need to apply a TPS transformation. Indeed the TPS of the worst template, the Random model, provides the best improvement ($p = 1.8 \times 10^{-12}$) and, on the other hand, the best head model, the Average Surface, is not significantly improved ($p = 0.25$).

Although the Average Surface model is significantly better than the CHBM-305 TPS model from a statistical point of view ($p = 0.03$), this improvement in localization errors is scarce in practical terms. However, the former provides a valuable advantage since there is no need to measure the individual electrode positions.

3.3. The possible effect of the imperfect anatomical correspondence of cortical surfaces

The MLE of most of the approximate head models is around 6 mm despite the different shape approximations adopted. We suspect that although improving shape is mandatory, another cause of localization error, common to all models, should be dealt with in the future. It should be noted that, even for the best of the surface registration methods, the perfect anatomical correspondence between cortices cannot be achieved since all subjects have unavoidable differences in the sulci/gyri disposition. Therefore, for example, the cortices of both Average Surface (which results to be smoother than the individual one) and Random models present anatomical locations that lack meaningful correspondence in the actual individual cortex. We believe this is the cause of the com-

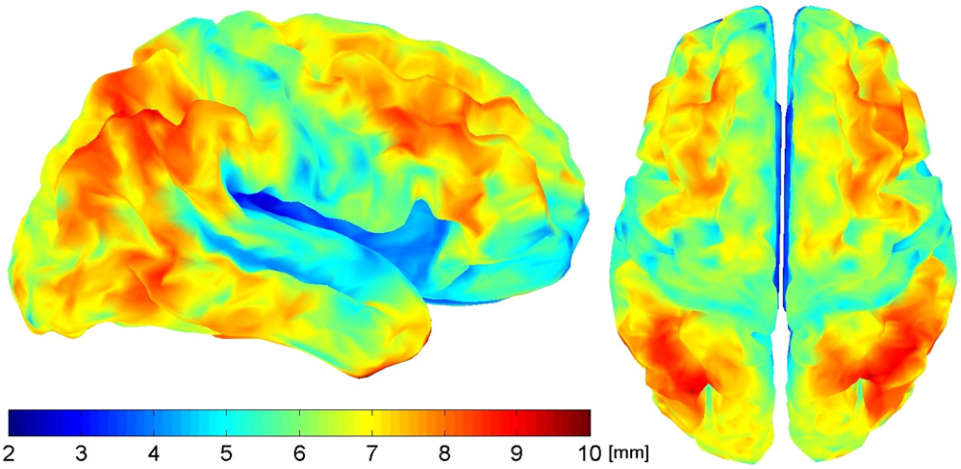

Fig. 3. Average localization error among the 305 subjects for each source location. It can be seen that this error is lower for deeper sources, and higher for sources near the inskull.

mon baseline of localization error in the tested approximate head models.

To test this hypothesis we created a new set of "false" head models with their cortical surfaces in perfect anatomical correspondence. This was achieved by warping the MNI-27 cortical surface to each individual space with the nonlinear transformation estimated to create the inskulls (see Section 2). This approach is inspired in a previous work for MEG Forward and Inverse solutions (Mattout et al., 2007). In that work, cortex models are built by warping a canonical mesh to individual space by a diffeomorphism. One of their objectives was precisely ensuring anatomical correspondence between individual meshes, as well as with a canonical one.

The MLE and q95 were much lower for the "false" head models: 0.55 mm and 5.08 mm respectively. This clearly supports the detrimental effect on source localization of the imperfect anatomical correspondence between the cortices used to asses approximate head models. This is in apparent contrast to (Mattout et al., 2007; Henson et al., 2009) where the performance of a warped canonical mesh for MEG source localization is comparable to that of the actual individual's anatomical mesh. However in our case the comparison in not between different proposals (actual or canonical) of the individual's cortical model; but between different approximate head models constructed from a MRI database.

4. Discussions and conclusions

We presented several approximate head models that could be used in ESI when the head model based on the actual MRI of the individual is not available. This is a problem that has already been addressed in the literature in the past. One of the first attempts used approximate models based on the standard MNI-shaped MRIs (Fuchs et al., 2002), such as the ICBM-152 or MNI-27 average heads. Recently Darvas et al. proposed a Thin Plate Spline transformation to warp this type of models (in particular the ICBM-152) to the individual's space, based on matching both the individual's and template's electrode positions (Darvas et al., 2006).

The MNI-shaped models are not representative, in the sense of shape, of the target population, and the TPS approach depends on electrode measurement and template quality, with accuracy only reliable at the closest places of the scalp. Therefore we propose new head models that are more representative of the target population. These are Average Surfaces and Average Lead Field. We adopted head models based on surfaces since we are interested only in evaluating an improvement in shape approximation.

Our first conclusion is that the lead field of an approximate head model should not be constructed with the source moments constrained to be normal to the cortical surface, since this yields smaller localization errors. This can be explained since there might be a large difference in both the actual and approximate normal direction, even when anatomical correspondence is achieved.

Nevertheless, we believe that the largest cause of localization error is the imperfect anatomical correspondence between cortices. This might be due to (1) the unavoidable inter-individual differences in the human cortex and (2) the inaccuracy of the registration methods. We think that overcoming the second issue by defining newer anatomical correspondence criteria specifically tailored to decrease the localization error might improve the performance of our proposed average approximate head models.

The Average Surface (which, as demonstrated, is the estimate of the shape centroid of the target population) and the Average Lead Field significantly outperformed the MNI-shaped and Random model. As shown in Fig. 3 the localization error for our average models is lower for deeper sources while higher for sources near the skull. A classification by race, gender or head size before averaging, does not improve ESI.

Although our average models are not remarkably better than Darvas's CHBM-TPS model, they provide the advantage of not requiring the measurement of electrode positions which has to be done either by hand (de Munck et al., 1991) or by using a Polhemus device (Lamm et al., 2001). We speculate that the differences between the performance of centroid head models and either MNI-shaped or TPS-MNI models might be even larger for FEM/FDM models since this type of head modeling is probably much more sensitive to the approximations achieved at finer levels of detail of the image. This is beyond the scope of this paper and has to be tested in future work. A separate conclusion is that TPS models are not necessary if the template model is good enough.

Finally we acknowledge that a very promising line of research is to evaluate the Bayesian evidence of different approximate head models in the context of ESI. The evidence could be used for selecting an optimal approximate head model as (Henson et al., 2009) did for individual ones or for Bayesian Model Averaging (BMA) (Trujillo-Barreto et al., 2004) of head models.

In this regard we introduce an approximate to BMA of head models: the Average Lead Field, which represents a promising tool for ESI when the individual's MRI is not available. We think that the Average Lead Field might be the appropriate approach when adopting any type of head modeling since it only needs a rough alignment between individual MRIs prior its calculation. This model can be used in large clinical studies where the electrode montage is predetermined.

Acknowledgements

We thank to all the members of the Cuban Human Brain Mapping Project (which is a project of the Cuban Health Care System) and especially to technicians Joe Michel Lopes Inguanzo and Rogney Marine Isalgue who made possible the acquisition of the MR data for healthy subjects. We also thank to Prof. Alan Evans and his group from the Montreal Neurological Institute for providing us the tools necessary for surface extraction and registration. This work was funded in part by the SECyT(Argentina)-CITMA(Cuba) Bilateral Cooperation Project CU/PA/03-SV/022. The work of N.v.E, S.K. and C.H. was partly funded by CONICET, CICpBA and ANPCyT PICT 2007-00535 and 2006-35423.

Appendix A. The Average Surface model: the centroid estimate

The Average Surface model is intended to be an estimate of the shape centroid of the target population. This is based on $N = 305$ MRIs randomly sampled from the Cuban Population. A proposal for the estimation of the centroid of a set of MRIs can be found in (Guimond, 2000). It consists of averaging all images after registering them all to a single individual, arbitrarily chosen from the set. This average is then warped with the average of the estimated registration transformations. To achieve a highly detailed image, these transformations have to be nonlinear and high dimensional. This method, as well as others in the literature (Kochunov et al., 2001; Christensen et al., 2006), is computationally demanding and not easy to update.

The steps followed in (Guimond, 2000) to calculate the centroid MRI estimate, A($\mathbf{x}$), being $\mathbf{x}$ the coordinate variable, can be written in a single step:

$$A(\mathbf{x}) = \sum_{j=1}^{N} I_j(\mathbf{h}_j(\mathbf{x})),$$
$$\mathbf{h}_j(\mathbf{x}) = \mathbf{t}_j \cdot \left(\sum_{m=1}^{N} \mathbf{t}_m \right)^{-1} (\mathbf{x}), \tag{3}$$

where $I_j(\mathbf{x})$ and $\mathbf{t}_j(\mathbf{x})$, for $j = 1,\ldots,305$, are the individual MRIs and nonlinear transformations respectively. The set of surfaces, S_j, of the same type, e.g. inskull, can be submitted to the same procedure to obtain the centroid surface estimate:

$$\tilde{S}_j = \mathbf{h}_j^{-1}(S_j),$$
$$S_{\mathrm{A}} = \sum_{j=1}^{N} \tilde{S}_j^{\mathrm{SH}}, \quad (4)$$

where $\tilde{S}_j^{SH}$ is the SH representation of the warped surface $\tilde{S}_j$.

In this work we applied this algorithm to obtain the estimate of our head model centroid rigorously. The nonlinear high dimensional registration method is described in (Thirion, 1998). We aligned the surfaces of the average centroid model, as obtained with Eq. (4), to the fiducial-based system, and represented them with the SH expansion. This allowed us to compare the surface centroid estimate with the Average Surface model by calculating the distance between their corresponding surfaces using Eq. (2). These were 1.54 mm, 0.90 mm, 0.90 mm, 0.92 mm for cortex, inskull, outskull and scalp respectively. These values are very low compared to the differences between true and approximate models in this work; they also yield to almost identical localization errors in ESI. This justifies the use of a simple surface averages (the Surface Average model) as an estimate of the centroid shape of the target population.

References

Abramovitz M, Stegun IA. Handbook of mathematical functions. New York: Dover Pubications; 2009. p. 1970.

Ad-Dab'bagh Y, Lyttelton O, Muehlboeck JS, Lepage C, Einarson K, Mok K, et al. The CIVET image processing environment: a fully automated comprehensive pipeline for anatomical neuroimaging research. In: Proceedings of the 12th annual meeting of the organization for human brain mapping. NeuroImage; 2006.

Ashburner J, Friston KJ. Nonlinear spatial normalization using basis functions. Human Brain Mapping 1999;7:254–66.

Christensen GE, Johnson HJ, Vannier MW. Synthesizing average 3D anatomical shapes. Neuroimage 2006;32:146–58.

Collins DL, Zijdenbos AP, Kollokian V, Sled JG, Kabani NJ, Holmes CJ, et al. Design and construction of a realistic digital brain phantom. IEEE Transactions on Medical Imaging 1998;17:463–8.

Dale AM, Sereno MI. Improved localization of cortical activity by combining EEG and meg with mri cortical surface reconstruction: a linear approach. Journal of Cognitive Neuroscience 1993;5:162–76.

Darvas F, Ermer JJ, Mosher JC, Leahy R. Generic head models for atlas-based EEG source analysis. Human Brain Mapping 2006;27:129–43.

de Munck JC. A linear discretization of the volume conductor boundary integral-equation using analytically integrated elements. IEEE Transactions on Biomedical Engineering 1992;39:986–90.

de Munck JC, Peters MJ. A fast method to compute the potential in the multisphere model. IEEE Transactions on Biomedical Engineering 1993;40:1166–74.

de Munck JC, Vijn PCM, Spekreijse Henk. A practical method for determining electrode positions on the head. Electroencephalography and Clinical Neurophysiology 1991;78:85–7.

Ermer JJ, Mosher JC, Baillet S, Leahy RM. Rapidly recomputable EEG forward models for realistic head shapes. Physics in Medicine and Biology 2001;46:1265–81.

Fuchs M, Drenckhahn R, Wischmann HA, Wagner M. An improved boundary element method for realistic volume-conductor modeling. IEEE Transactions on Biomedical Engineering 1998;45:980–97.

Fuchs M, Kastner J, Wagner M, Hawes S, Ebersole J. A standardized boundary element method volume conductor model. Clinical Neurophysiology 2002;113:702–12.

Fuchs M, Wagner M, Kastner J. Boundary element method volume conductor models for EEG source reconstruction. Clinical Neurophysiology 2001;112:1400–7.

Guimond A. Average brain models: a convergence study. Computer Vision and Image Understanding 2000;77:192–210.

Hämäläinen M, Sarvas J. Realistic conductivity geometry modelof the human head for interpretation of neuromagnetic data. IEEE Transactions on Biomedical Engineering 1989;36:165–71.

Haueisen J, Bttner A, Funke M, Brauer H, Nowak H. Influence of boundary element discretization on the forward and inverse problem in electroencephalography and magnetoencephalography. Biomedizinische Technik 1997;42:248.

Henson RNA, Mattout J, Friston KJ. Selecting forward models for MEG source-reconstruction using model-evidence. Neuroimage 2009;46:168.

Huiskamp G, Vroeijenstijn M, van Dijk R, Wieneke G, van Huffelen AC. The need for correct realistic geometry in the inverse EEG problem. IEEE Transactions on Biomedical Engineering 1999;46:1281–7.

Jenkinson M, Pechaud M, Smith S. BET2: MR-based estimation of brain, skull and scalp surfaces. In: Eleventh annual meeting of the organization for human brain mapping; 2005.

Kochunov P, Lancaster JL, Thompson P, Woods R, Mazziotta J, Hardies J, et al. Regional spatial normalization: toward an optimal target. Journal of Computer Assisted Tomography 2001;25:805–16.

Lamm C, Windischberger C, Leodolter U, Moser E, Bauer H. Co-registration of EEG and MRI data using matching of spline interpolated and MRI-segmented reconstructions of the scalp surface. Brain Topography 2001;14:93–9.

Le J, Lu M, Pellouchoud E, Gevins A. A rapid method for determining standard 10/10 electrode positions for high resolution EEG studies. Electroencephalography and Clinical Neurophysiology 1998;106:554–8.

Malmivuo J, Plonsey R. Bioelectromagnetism—principles and applications of bioelectric and biomagnetic fields. Oxford University Press; 1995.

Mattout J, Henson RNA, Friston KJ. Canonical source reconstruction for MEG. Computational Intelligence and Neuroscience 2007;2007:67613.

Mazziotta J, et al. A probabilistic atlas and reference system for the human brain: International Consortium for Brain Mapping. (ICBM). Philosophical Transactions of the Royal Society of London Series B: Biological Sciences 2001;356:1293–322.

Meijs JWH, Weier OW, Peters MJ, vanOosterom A. On the numerical accuracy of the boundary element method. IEEE Transactions on Biomedical Engineering 1989;36:1038–49.

Neilson L. Realistic head volume conductor modeling for EEG source localization. University of Alberta; 2003.

Oostendorp TF, Delbeke J, Stegeman DF. The conductivity of the human skull: results of in vivo and in vitro measurements. IEEE Transactions on Biomedical Engineering 2000;47:1487–92.

Pascual-Marqui RD. Standardized low resolution brain electromagnetic tomography (sLORETA): technical details. Methods & Findings in Experimental & Clinical Pharmacology 2002;24D:5–12.

Robbins SM. Anatomical standardization of the human brain in euclidean 3-space and on the cortical 2-manifold. Montreal: School of Computer Science, McGill University; 2003.

Shattuck D, Leahy R. Brainsuite: an automated cortical surface identification tool. Medical Image Analysis 2002;6:129–42.

Thirion JP. Image matching as a diffusion process: an analogy with Maxwell's demons. Medical Image Analysis 1998;2:243–60.

Trujillo-Barreto NJ, Aubert-Vazquez E, Valdés-Sosa PA. Bayesian model averaging for EEG/MEG imaging. Neuroimage 2004;21:1300–19.

Trujillo-Barreto NJ, Aubert-Vazquez E, Penny WD. Bayesian M/EEG source reconstruction with spatio-temporal priors. Neuroimage 2008;39:318–35.

van't Ent D, de Munck JC, Kaas AL. A fast method to derive realistic BEM models for E/MEG source reconstruction. IEEE Transactions on Biomedical Engineering 2001;48:1434–43.

von Ellenrieder N, Muravchik CH, Nehorai A. Effects of geometric head model perturbations on the EEG forward and inverse problems. IEEE Transactions on Biomedical Engineering 2006;53:421–9.

von Ellenrieder N, Muravchik CH, Wagner M, Nehorai A. Effect of head shape variations among individuals on the EEG/MEG forward and inverse problems. IEEE Transactions on Biomedical Engineering 2009;56:587–97.

Wang YH, Gotman J. The influence of electrode location errors on EEG dipole source localization with a realistic head model. Clinical Neurophysiology 2001;112:1777–80.

Wendel K, Malmivuo J. Correlation between live and post mortem skull conductivity measurements. Proceedings of the 28th Annual International Conference of the IEEE Engineering in Medicine and Biology Society 2006;1:4285–8.

Wolters CH, Anwander A, Tricoche X, Weinstein D, Koch MA, McLeod RS. Influence of tissue conductivity anisotropy on EEG/MEG field and return current computation in a realistic head model: a simulation and visualization study using high-resolution finite element modeling. Neuroimage 2006;30:813–26.

Zhang YC, van Drongelen W, He B. Estimation of in vivo brain-to-skull conductivity ratio in humans. Applied Physics Letters 2006;89:223903.